

Article

Development and characterization of a fluorescent tracer for the free fatty acid receptor 2 (FFA2/GPR43)

Anders Højgaard Hansen, Eugenia Sergeev, Sunil K. Pandey, Brian D. Hudson, Elisabeth Christiansen, Graeme Milligan, and Trond Ulven

J. Med. Chem., **Just Accepted Manuscript** • Publication Date (Web): 01 Jun 2017

Downloaded from <http://pubs.acs.org> on June 1, 2017

Just Accepted

“Just Accepted” manuscripts have been peer-reviewed and accepted for publication. They are posted online prior to technical editing, formatting for publication and author proofing. The American Chemical Society provides “Just Accepted” as a free service to the research community to expedite the dissemination of scientific material as soon as possible after acceptance. “Just Accepted” manuscripts appear in full in PDF format accompanied by an HTML abstract. “Just Accepted” manuscripts have been fully peer reviewed, but should not be considered the official version of record. They are accessible to all readers and citable by the Digital Object Identifier (DOI®). “Just Accepted” is an optional service offered to authors. Therefore, the “Just Accepted” Web site may not include all articles that will be published in the journal. After a manuscript is technically edited and formatted, it will be removed from the “Just Accepted” Web site and published as an ASAP article. Note that technical editing may introduce minor changes to the manuscript text and/or graphics which could affect content, and all legal disclaimers and ethical guidelines that apply to the journal pertain. ACS cannot be held responsible for errors or consequences arising from the use of information contained in these “Just Accepted” manuscripts.

1
2
3
4
5
6
7
8
9
10
11
12
13
14
15
16
17
18
19
20
21
22
23
24
25
26
27
28
29
30
31
32
33
34
35
36
37
38
39
40
41
42
43
44
45
46
47
48
49
50
51
52
53
54
55
56
57
58
59
60

Development and characterization of a fluorescent tracer for the free fatty acid receptor 2 (FFA2/GPR43)

*Anders Højgaard Hansen^{†,§}, Eugenia Sergeev^{‡,§}, Sunil K. Pandey[†], Brian D. Hudson[‡], Elisabeth
Christiansen[†], Graeme Milligan[‡] and Trond Ulven^{†*}*

[†]Department of Physics, Chemistry and Pharmacy, University of Southern Denmark, Campusvej
55, DK-5230 Odense M, Denmark

[‡]Centre for Translational Pharmacology, Institute of Molecular, Cell and Systems Biology,
College of Medical, Veterinary and Life Sciences, University of Glasgow, Glasgow G12 8QQ,
Scotland, United Kingdom

1
2
3
4
5
6
7
8
9
10
11
12
13
14
15
16
17
18
19
20
21
22
23
24
25
26
27
28
29
30
31
32
33
34
35
36
37
38
39
40
41
42
43
44
45
46
47
48
49
50
51
52
53
54
55
56
57
58
59
60
ABSTRACT

The free fatty acid receptor 2 (FFA2/GPR43) is considered a potential target for treatment of metabolic and inflammatory diseases. Here we describe the development of the first fluorescent tracer for FFA2 intended as a tool for assessment of thermodynamic and kinetic binding parameters of unlabeled ligands. Starting with a known azetidine FFA2 antagonist, we used a carboxylic acid moiety known not to be critical for receptor interaction as attachment point for a nitrobenzoxadiazole (NBD) fluorophore. This led to the development of **4** (TUG-1609), a fluorescent tracer for FFA2 with favorable spectroscopic properties and high affinity, as determined by bioluminescence resonance energy transfer (BRET)-based saturation and kinetic binding experiments, as well as a high specific to non-specific BRET binding signal. A BRET-based competition binding assay with **4** was also established and used to determine binding constants and kinetics of unlabeled ligands.

1
2
3
4
5
6 INTRODUCTION
7

8 The free fatty acid receptor 2 (FFA2, also known as GPR43) is a 7-transmembrane receptor
9 activated by short-chain fatty acids (SCFAs) produced endogenously during colonic fermentation
10 of dietary fiber by the gut microbiota.¹⁻⁵ The receptor is expressed in various cell types such as
11 adipocytes and pancreatic β -cells.^{6,7} FFA2 is also expressed in immune cells, including
12 neutrophils, eosinophils, B lymphocytes, and peripheral blood mononuclear cells, and has been
13 shown to mediate SCFA-promoted chemotaxis in neutrophils.⁸⁻¹¹ In recent years FFA2 has
14 attracted much attention as a possible target for treatment of obesity,¹² inflammation,^{9,13,14} and
15 metabolic diseases.^{5,15} It has however frequently been unclear if the preferred mode of action
16 was agonism or antagonism.³ It has been shown that the loss of FFA2 and the related SCFA
17 receptor FFA3 (GPR41) leads to increased insulin secretion and improved glucose tolerance,
18 indicating a therapeutic potential of antagonists against metabolic diseases.⁷ The role of the
19 receptor in chemotaxis of neutrophils has also suggested anti-inflammatory potential of
20 antagonists. For example, the FFA2 antagonist GLPG0974 (**1**, Chart 1) has been demonstrated to
21 inhibit human neutrophil recruitment *in vitro* and *in vivo*, suggesting that the compound could
22 represent a potential therapeutic target for treatment of inflammatory diseases.^{13,16} Clinical trials
23 with **1** for treatment of ulcerative colitis indeed showed decreased neutrophil infiltration although
24 no significant improvement of symptoms was observed in the patients.¹⁷ To fully assess the
25 therapeutic potential of FFA2, high quality tool compounds are needed for further investigations
26 of FFA2 pharmacology and function.

27
28
29
30
31
32
33
34
35
36
37
38
39
40
41
42
43
44
45
46
47
48
49
50
51
52
53
54
55
56
57
58
59
60
Fluorescent tracer molecules have been established as useful tools for real-time monitoring of
receptor-ligand interactions and offer several advantages over conventional radioactive tracers.¹⁸⁻

1
2
3
4
5
6
7
8
9
10
11
12
13
14
15
16
17
18
19
20
21
22
23
24
25
26
27
28
29
30
31
32
33
34
35
36
37
38
39
40
41
42
43
44
45
46
47
48
49
50
51
52
53
54
55
56
57
58
59
60

²¹ The small, green-emitting fluorophore 4-amino-7-nitrobenzoxadiazole (NBD) has previously been employed for labeling small molecules, lipids and proteins and has been applied in competition binding assays and for imaging of living cells.²²⁻²⁵ The fluorescence of NBD is almost completely quenched in polar and protic solvents, whereas high fluorescence activity is preserved in non-polar environments, which can amplify signal to noise ratio for the bound NBD.²⁶ Bioluminescence resonance energy transfer (BRET) between a receptor tagged at its N-terminus with Nanoluciferase (NLuc) and a fluorescent ligand is useful for real-time interaction monitoring, also between GPCRs and small molecules.²⁷ We have recently taken advantage of the properties of NBD by developing two free fatty acid receptor 1 (FFA1) fluorescent tracers as well as a BRET competition binding assay to NLuc tagged FFA1 and demonstrated its usefulness for investigating the binding of natural and synthetic ligands to the FFA1 receptor.²¹ NBD was selected due to the almost perfect overlap between its absorption band and the emission band of NLuc. NBD is known to be prone to photobleaching.²⁸ However, the avoidance of an external light source in the BRET assay minimizes this problem. Recognizing the need for a similar fluorescent tracer and assay for FFA2, we aimed to follow an equivalent strategy for this receptor. We here report on the design, synthesis and characterization of the first fluorescent tracer for FFA2 and the use of the tracer in a BRET competition binding assay. The carboxylic acid chain of **1** was originally introduced to tackle ADME issues in the compound series.¹³ Although the carboxylate contributes somewhat to potency of the compound and has been demonstrated to depend on the presence of at least one of the two orthosteric arginine residues, the group is not required for the activity of the compound.²⁹ The closely related azetidine analogue **2** as well as its methyl ester (**3**) are also efficient FFA2 antagonists.^{13,29} As the carboxylic acid group appeared to be dispensable for the affinity of the compounds, we decided

to explore this group as attachment point for an NBD fluorophore in the design of the proposed FFA2 fluorescent tracer **4** (TUG-1609, Chart 1).

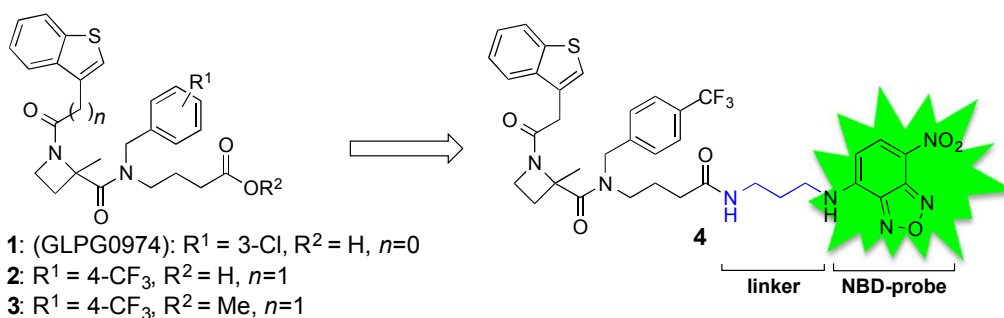
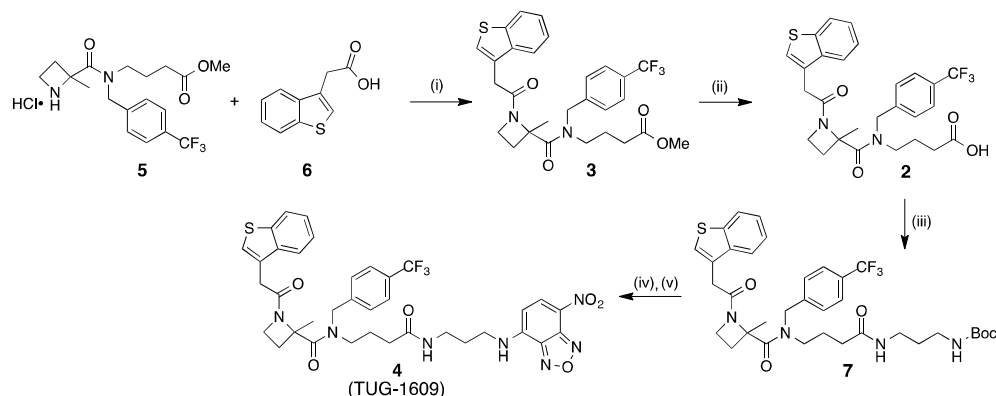


Chart 1. Design strategy for an antagonist-based FFA2 fluorescent tracer.

RESULTS AND DISCUSSION

Synthesis

The fluorescent tracer **4** was synthesized in 13 steps from commercial starting materials. Azetidine **5** was synthesized according to the procedures described by Pizzonero and co-workers (Scheme 1).¹³ Benzothiene-3-acetic acid **6** was activated with bis(2-oxo-3-oxazolidinyl)phosphinic chloride (BOP-Cl) and coupled with **5** to give **3**. Methyl ester **3** was hydrolyzed to carboxylic acid **2**, activated using BOP-Cl and coupled to mono-Boc-protected 1,3-diaminopropane to give **7**. Boc-deprotection afforded the crude amine, which was reacted directly with NBD-Cl in a nucleophilic aromatic substitution to give the fluorescent **4** in 47% yield after purification by preparative HPLC.²¹

Scheme 1. Synthesis of **4**.^a

^aReagents and conditions: (i) Et_3N , BOP-Cl, DCM, 80°C , 25 h, 40%; (ii) LiOH, THF, water, rt, 96%; (iii) a) Et_3N , BOP-Cl, DCM, 50°C , 3 h; b) Et_3N , *tert*-butyl (3-aminopropyl)carbamate, 30 min at 50°C , then rt overnight, 46%; (iv) TFA, DCM, rt; (v) NBD-Cl, NaHCO_3 , MeOH, 50°C , 4 h, 38% over 2 steps.

Characterization of Fluorescence Properties

Absorption and fluorescence spectra of **4** were recorded in $\text{PBS}_{7.4}$ and in *n*-octanol, with the latter solvent emulating the environment of a predominately hydrophobic receptor binding site or membrane.³⁰ A shift of 30 nm was observed when comparing the maximum excitation of **4** in *n*-octanol ($\lambda_{\text{max}} = 462 \text{ nm}$) with that in PBS buffer ($\lambda_{\text{max}} = 492 \text{ nm}$, spectrum not shown). The extinction coefficient (ϵ) of **4** at its maximum excitation wavelength was determined ($\epsilon_{462 \text{ nm}} = 12,550 \text{ M}^{-1} \text{ cm}^{-1}$) from absorption spectra recorded in *n*-octanol at increasing concentrations of **4** (Table 1). Fluorescent tracer **4** exhibits maximum emission at 525 nm with a Stokes shift of 63 nm and a quantum yield (Φ) of 0.62 in *n*-octanol (Table 1 and Figure 1A), whereas the fluorescence was almost absent in PBS (Figure 1B). Overall, **4** demonstrated properties comparable to the values observed for the recently reported NBD-based FFA1 tracers.²¹

Table 1. Absorption and fluorescence properties of **4**.^a

<i>n</i> -Octanol					PBS buffer (pH 7.4)	
λ_{ex} [nm]	λ_{em} [nm]	SS [nm]	$\epsilon_{462 \text{ nm}}^b$ [M ⁻¹ cm ⁻¹]	Φ^b	λ_{ex} [nm]	λ_{em} [nm]
462	525	63	12,550 ± 276	0.62 ± 0.012	492	557

^aSS, Stokes shift; Φ , quantum yield; ϵ , extinction coefficient. ^bValues are reported ± standard error (SE).

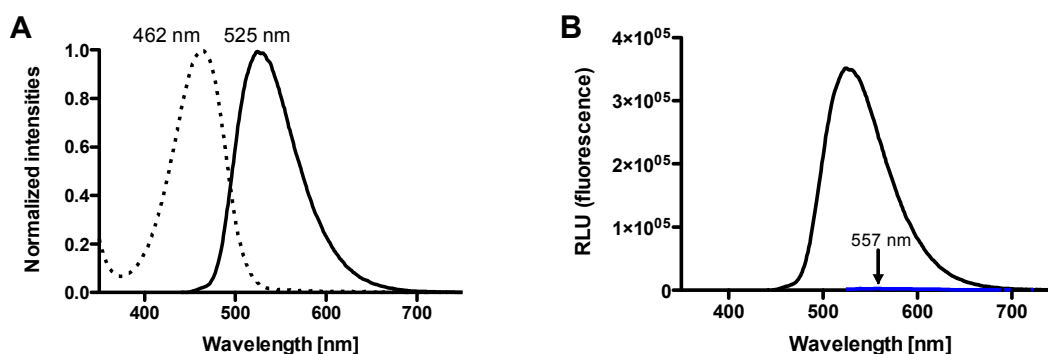


Figure 1. Absorption and fluorescence properties of **4**. A) Normalized absorption (dotted line) and fluorescence (solid line) spectra in *n*-octanol. B) Effect of solvent on fluorescence activity of **4** in *n*-octanol (black curve) and PBS buffer (blue curve, maximum indicated by arrow).

Functional Characterization of **4** on FFA2

Tracer **4** was found to act as an antagonist of propionate (C3)-mediated elevation of inositol monophosphate (IP1) levels in Flp-InTM T-RExTM 293 cells induced to express a form of human FFA2 that had enhanced Yellow Fluorescent Protein linked in frame to the intracellular C-terminal tail of the receptor (hFFA2-eYFP) (Figure 2A). The ability of **4** to inhibit the effects of an EC₈₀ concentration of C3 was similar to that of the related clinically tested FFA2 antagonist **1**

and analogue **2** (Figure 2A, Table 2). Furthermore, in membrane preparations derived from these cells, increasing concentrations of **4** were able to prevent specific binding of [³H]-**1** to the hFFA2-eYFP construct with affinity akin to that of unlabeled **1** and **2** (Figure 2B, Table 2).

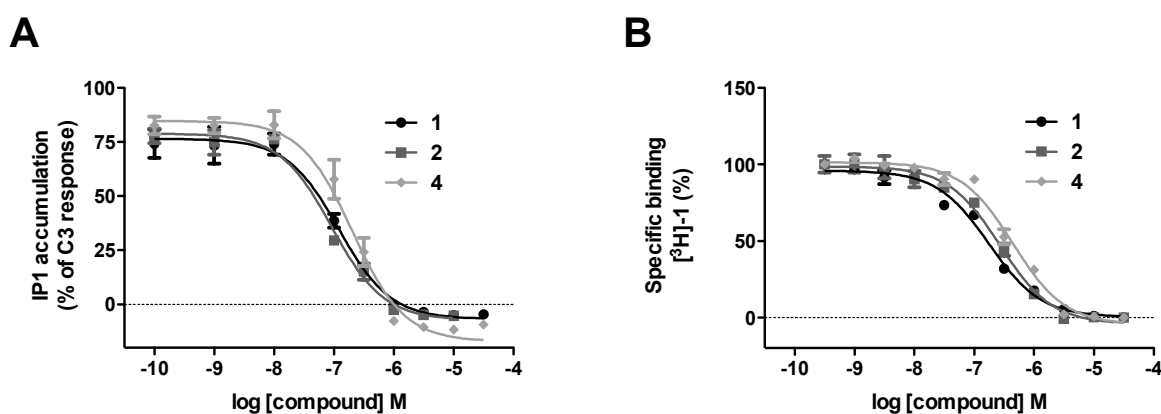


Figure 2. (A) Functional characterization of **4** against **1** and **2** in IP1 accumulation assay. (B) Displacement of [³H]-**1** using **1**, **2** and **4**. Error bars represent SE, n=3.

Table 2. Characterization of antagonist properties and affinities of unlabeled carboxylic acid **1**, methyl ester **2** and fluorescent tracer **4** as antagonist in functional IP1 and radioligand displacement assays.

Cmpd	pIC ₅₀ (IP1) ^a	pK _i (Displacement) ^b
1	6.94 ± 0.04	7.76 ± 0.11
2	7.08 ± 0.05	7.64 ± 0.08
4	6.57 ± 0.10	7.31 ± 0.06

^aThe ability of **4** to inhibit IP1 accumulation at EC₈₀ concentration of propionate. ^bK_i was determined in [³H]-**1** displacement assays. Values are means ± SE, n=3.

Characterization of **4** as an FFA2 Tracer Molecule

A saturation binding experiment was performed by adding varying concentrations of **4** to membrane preparations generated from Flp-InTM T-RExTM 293 cells induced to express hFFA2-eYFP. This allowed BRET (Figure 3A) between NLuc and the NBD domain of bound **4**. Subtraction of signal obtained when the same concentrations of **4** were co-incubated with 50 μ M **1** was used to define non-specific binding of **4** (Figure 3A) and to generate a monophasic binding curve with an estimated K_d for **4** of 65.1 ± 1.8 nM (Figure 3B). Following addition of 100 nM **4** to membrane preparations and waiting 2 hours to allow binding to reach equilibrium, wash-out of unbound **4** allowed the dissociation of **4** to be monitored under conditions of infinite dilution by the reduction of specific BRET signal over time (Figure 3C). The tendency of the signal to extrapolate below zero in Figure 3C may be due to depletion of substrate for NLuc at the end of the longer measurements. Time courses of development of specific BRET signals following addition of different concentrations of **4** showed the estimated ligand association rate to increase with ligand concentration as predicted by mass action (Figure 3D). These experiments allowed the determination of a dissociation rate k_{off} of 0.0249 ± 0.0009 min⁻¹ and an association rate k_{on} of $368,000 \pm 29300$ M⁻¹ min⁻¹ for tracer **4**. Using these constants to independently calculate the affinity of **4** yielded a K_d of 67.7 nM, a value very close to that obtained from the saturation binding experiment.

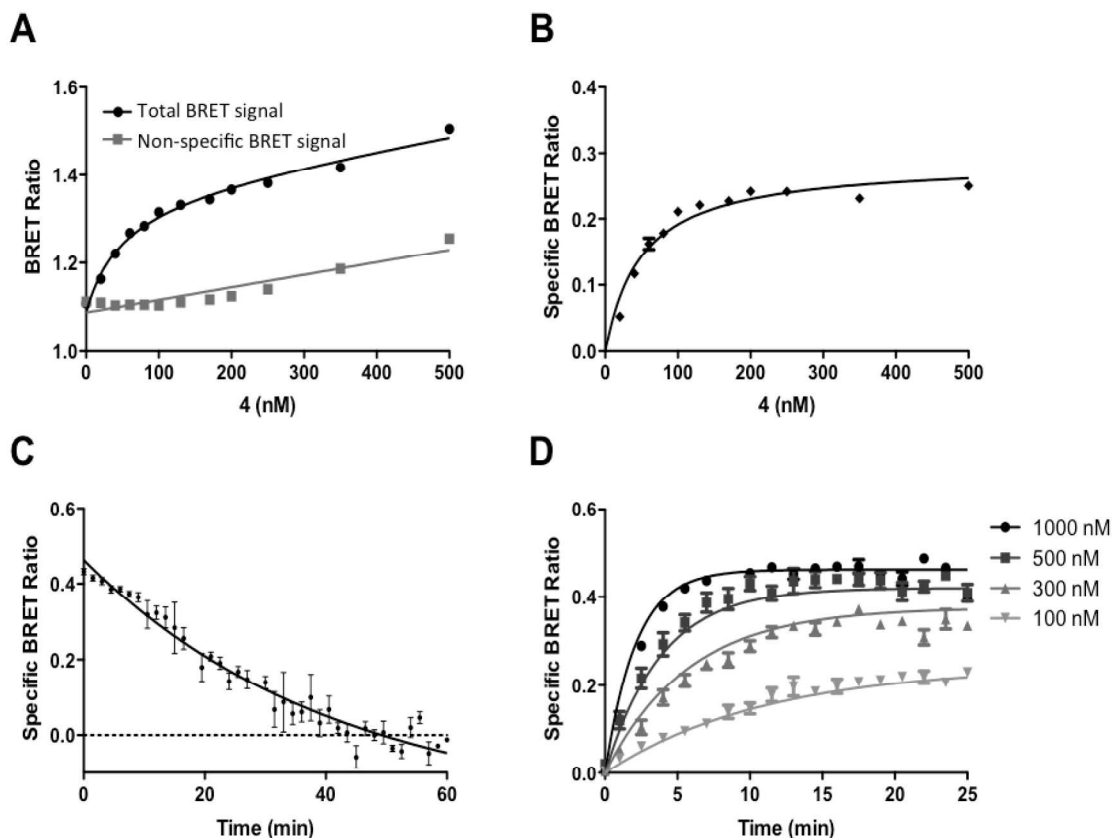
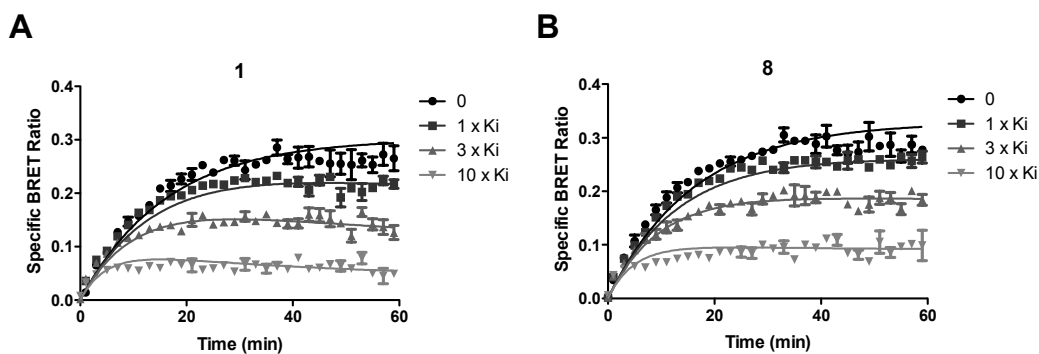


Figure 3. (A) BRET-based saturation binding experiment of tracer **4** bound to NLuc tagged FFA2 (total binding signal); BRET between **4** and NLuc tagged FFA2 recorded using non-fluorescent **1** at high concentration (10 μ M) (non-specific binding signal). (B) Monophasic binding curve for **4** obtained by subtracting total binding signal from non-specific binding signal of **4**. (C) Dissociation of **4** monitored under conditions of infinite dilution (asymptote at -0.17 ± 0.02). (D) Time courses measuring the association of **4** to NLuc tagged FFA2 at varying concentrations of **4**. Error bars represent SE, $n=3$.

To compare the usefulness of **4** with that of the radiolabeled FFA2 antagonist [3 H]-**1**, we employed the BRET signal produced by **4** bound specifically to NLuc tagged FFA2 in the presence of varying concentrations of either **1** or the FFA2 antagonist CATPB (**8**) as a means to

1
2
3 concomitantly measure both ‘on’ and ‘off’ rates of these unlabeled ligands (Table 3).³¹
4
5 Antagonist **8** is structurally different from **1** but is known to bind to the same site at the FFA2
6 receptor.^{29,32} Previous studies using [³H]-**1** indicated that although these two compounds have
7 similar affinity at human FFA2, **8** is relatively ‘fast on-fast off’ whilst **1** displays both slower
8 association and slower dissociation kinetics.²⁹ These features were reproduced and confirmed
9 when employing **4** in such binding kinetic analyses (Figure 4). The rate constants corresponded
10 to dissociation constants of 46.9 nM and 18.9 nM for **1** (Figure 4A) and **8** (Figure 4B),
11 respectively (Table 3). No problems related to bleaching or day-to-day variability was noticed
12 using the BRET assay when care was taken to protect the compound from unnecessary exposure
13 to light.
14
15
16
17
18
19
20
21
22
23
24
25
26
27



28
29
30
31
32
33
34
35
36
37
38
39
40
41 **Figure 4.** Application of **4** in binding kinetic analyses of unlabeled ligands; (A) **1**, (B) **8**. Error
42 bars represent SE, n=3.
43
44
45
46
47
48
49
50
51
52
53
54
55
56
57
58
59
60

Table 3. Kinetic properties for fluorescent tracer **4** and unlabeled ligands **1** and **8**.

Cmpd	k_{off} (min^{-1})	k_{on} ($\text{M}^{-1} \text{min}^{-1}$)	K_{d} (nM)
4 ^a	0.0249 ± 0.0009	$368,000 \pm 29,300$	67.7 ± 5.9
1 ^b	0.0099 ± 0.0014	$211,000 \pm 4,780$	46.9 ± 6.7
8 ^b	0.0205 ± 0.0010	$1,083,000 \pm 59,800$	18.9 ± 1.4

^aRate constants and dissociation constant of **4** determined in BRET-based saturation binding assay. ^bRate constant and dissociation constants for unlabeled ligands **1** and **8** determined using tracer **4** in BRET-based competition binding assay. Values are means \pm SE, n=3.

Importantly, when varying concentrations of **4** were co-added with a range of concentrations of **1**, analysis of the binding of **4**, as reported by the specific BRET signal, was consistent with competition between the ligands to bind to the receptor (Figure 5A). Higher concentrations of **4** required increasing concentrations of **1** to compete for the receptor binding site (Figure 5A, Table 4). Equivalent conclusions were reached for **8** (Figure 5B) and provided an estimated affinity for human FFA2 of 14.5 nM, almost identical to the value determined previously when employing [³H]-**1**.²⁹ Notably, affinity values for **1** and **8** determined using **4** in competition binding experiments (Table 4) were found to be internally consistent with dissociation constants obtained when using **4** in binding kinetic analyses (Table 3). To be useful as a ligand with which to screen novel chemical ligands for affinity at human FFA2, it is important that employing **4** should result in ligand SAR as anticipated from other studies. It is known that replacement of the carboxylate moiety of **8** by methyl ester (**9**) reduces affinity at hFFA2 by more than 10 fold.²⁹ Herein, using **4** this expectation was again fulfilled (Figure 5C) with **9** displaying 23.6 fold lower affinity for human FFA2, when compared to **8**.

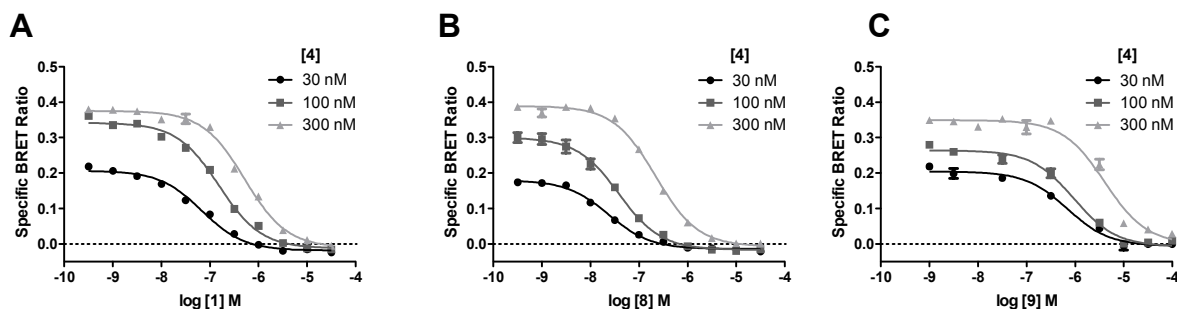
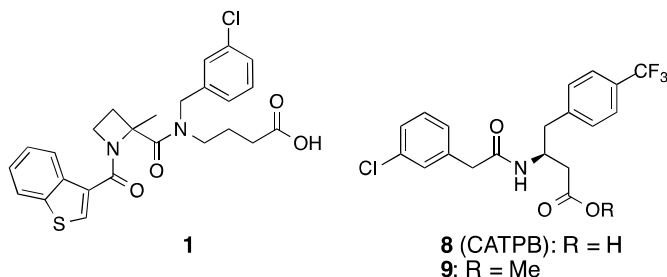


Figure 5. Application of **4** in competition binding experiments of unlabeled ligands (A) **1**, (B) **8**, (C) **9**. Error bars represent SE, $n=3$.

Table 4. Competition binding affinities of selected FFA2 antagonists.



		1	8	9
Affinity ^a	pK_i	7.16 ± 0.06	7.84 ± 0.04	6.42 ± 0.03
	K_i (nM)	69.2	14.5	380

^a Values for pK_i are means \pm SE, $n=3$.

CONCLUSION

By taking advantage of SAR information on known antagonists for FFA2, the fluorescent tracer molecule **4** was developed. Tracer **4** contains an NBD fluorescent probe and exhibits desirable spectroscopic properties, including a Stokes shift of 63 nm, low fluorescence activity in

1
2
3 aqueous solution, and a high quantum yield in non-polar environments. Using an NLuc construct
4 built into the extracellular N-terminal domain of the FFA2 receptor and BRET-based binding
5 experiments, tracer **4** was found to exhibit a K_d of 65 nM and a low non-specific binding signal.
6
7
8 The BRET binding assay with **4** was further applied to determine thermodynamic and kinetic
9
10 binding parameters of unlabeled FFA2 ligands, resulting in values comparable to those obtained
11
12 previously using a radiolabeled ligand. Compound **4** is the first fluorescent tracer for FFA2 and
13
14 is expected to be useful tool for further studies of the receptor as well as for characterization of
15
16 FFA2 ligands.
17
18
19
20
21
22
23

24 EXPERIMENTAL SECTION

25 26 27 **Synthesis**

28
29 Commercial starting materials and solvents were used without further purification, unless
30 otherwise stated. THF was freshly distilled from sodium/benzophenone, and MeOH and DCM
31 were dried over 3 Å sieves. Petroleum ether (PE) refers to alkanes with pb 60 – 80 °C. TLC was
32 performed on TLC silica gel 60 F254 plates and visualized at 254 or 365 nm or by staining with
33 ninhydrin or KMnO₄ stains. Purification by flash chromatography was carried out using silica gel
34 60 (0.040-0.063 mm, Merck). ¹H and ¹³C NMR spectra were recorded at 400 and 101 MHz,
35 respectively, on a Bruker Avance III 400 at 300 K. Rotamer peaks have been assigned by
36 asterisk (*). Integrals reported as H represent sum of rotamers, whereas integrals reported as H'
37 and H'' represent specific rotamers where H' + H'' = H for the relevant signal. High-resolution
38 mass spectra (HRMS) were obtained on a Bruker micrOTOF-Q II (ESI). Purity was determined
39 by HPLC and confirmed by inspection of NMR spectra (¹H and ¹³C NMR). HPLC analysis was
40 performed using a Gemini C18 column (5 μm, 4.6x150 mm); flow: 1 mL/min; 10% MeCN in
41
42
43
44
45
46
47
48
49
50
51
52
53
54
55
56
57
58
59
60

1
2
3 water (0-1 min), 10-100% MeCN in water (1-10 min), 100% MeCN (11-15 min), with both
4
5 solvents containing 0.1% HCOOH as modifier; UV detection at 254 nm. All test compounds
6
7 were of $\geq 95\%$ purity unless otherwise stated.
8
9

10 Compounds **1**, **8** and **9** were synthesized according to published procedures.^{13,33}

11
12 **4-(1-(2-(Benzo[*b*]thiophen-3-yl)acetyl)-2-methyl-*N*-(4-(trifluoromethyl)benzyl)azetidino-**
13
14 **2-carboxamido)butanoic acid (2)**. Compound **3** (50.0 mg, 92 μmol) dissolved in THF (1 mL)
15
16 was added 0.6 M aqueous LiOH (0.45 mL) and stirred for 3.5 h at rt, whereafter the reaction
17
18 mixture was acidified with 1 M HCl until pH 2-3 and extracted with EtOAc (x3). The extract
19
20 was washed with brine, dried over Na_2SO_4 , and concentrated *in vacuo* to give **2** as a sticky oil
21
22 (46.9 mg, 96%); ^1H NMR (400 MHz, CDCl_3) δ 7.93 – 7.51 (m, 4H), 7.49 – 7.13 (m, 5H), 4.93 –
23
24 4.26 (m, 2H), 4.09 – 2.95 (m, 6H), 2.61 – 2.43 (m, 1H), 2.40 – 2.12 (m, 3H), 2.00 – 1.70 (m,
25
26 5H); ^{13}C NMR (101 MHz, CDCl_3) δ 172.6, 170.2, 140.31, 140.25, 139.3, 138.8, 130.1, 129.9,
27
28 128.0, 127.0, 125.8, 124.6, 124.3, 124.1, 124.0, 122.9, 122.8, 122.2, 122.0, 121.8, 71.3, 46.7,
29
30 46.2, 43.3, 34.3, 33.6, 30.5, 29.8, 29.5, 29.0, 25.3, 23.7; ESI-HRMS calcd for $\text{C}_{27}\text{H}_{27}\text{F}_3\text{N}_2\text{NaO}_4\text{S}$
31
32 ($\text{M} + \text{Na}^+$) 555.1536, found 555.1544; HPLC: $t_{\text{R}} = 11.80$ min, 97.1% pure. ^1H NMR in overall
33
34 agreement with literature.¹³
35
36
37
38
39

40
41 **Methyl 4-(1-(2-(benzo[*b*]thiophen-3-yl)acetyl)-2-methyl-*N*-(4-(trifluoromethyl)benzyl)-**
42
43 **azetidino-2-carboxamido)butanoate (3)**. In a dry microwave vial carboxylic acid **6** (57.4 mg,
44
45 0.30 mmol) and amine **5** (93.4 mg, 0.23 mmol) were suspended in dry DCM (0.45 mL). To the
46
47 stirred suspension were added Et_3N (175 μL , 1.26 mmol) and BOP-Cl (88.5 mg, 0.35 mmol),
48
49 and the vial was heated at 80 $^\circ\text{C}$ for 25 h. The reaction was cooled to rt, vented, water was added,
50
51 and the mixture extracted with DCM (x5). The extract was dried over Na_2SO_4 and concentrated
52
53 *in vacuo*. The product was obtained after flash chromatography (EtOAc:PE 4:1 \rightarrow 100% EtOAc)
54
55
56
57
58
59
60

1
2
3 as a pale yellow sticky oil (50.2 mg, 40%): $R_f = 0.26$ (EtOAc); ^1H NMR (400 MHz, CDCl_3) δ
4 7.95 – 7.53 (m, 4H), 7.50 – 7.12 (m, 5H), 4.94 – 4.26 (m, 2H), 4.10 – 2.96 (m, 6H), 3.66* (s,
5 3H'), 3.63 (s, 3H''), 2.63 – 2.46 (m, 1H), 2.43 – 2.14 (m, 3H), 2.00 – 1.71 (m, 5H); ^{13}C NMR
6 (101 MHz, CDCl_3) δ 172.6, 172.0, 169.7, 141.4, 140.3, 139.3, 138.8, 130.1, 128.0, 126.9, 126.3,
7 125.8, 124.5, 124.3, 124.1, 124.0, 123.8, 122.9, 122.8, 122.1, 121.8, 71.0, 51.9, 51.8, 46.7, 46.3,
8 43.1, 34.4, 33.7, 31.3, 30.7, 29.4, 29.1, 23.8, 23.1; ESI-HRMS calcd for $\text{C}_{28}\text{H}_{29}\text{F}_3\text{N}_2\text{NaO}_4\text{S}$ ($\text{M} +$
9 Na^+) 569.1692, found 569.1714.
10
11
12
13
14
15
16
17
18
19

20 **1-(2-(Benzo[*b*]thiophen-3-yl)acetyl)-2-methyl-*N*-(4-((3-((7-nitrobenzo[*c*][1,2,5]oxadiazol-
21 4-yl)amino)propyl)amino)-4-oxobutyl)-*N*-(4-(trifluoromethyl)benzyl)azetidine-2-
22 carboxamide (4).** To a pre-dried microwave vial at rt, the Boc-protected amine **7** (23.9 mg, 35
23 μmol) was dissolved in dry DCM (70 μL) followed by dropwise addition of TFA (66 μL , 0.87
24 mmol). Upon full deprotection indicated by TLC the reaction mixture was diluted with DCM,
25 added NaHCO_3 (sat), extracted with DCM (x5), the organic phases dried over Na_2SO_4 , and
26 concentrated *in vacuo*. The crude amine (17 mg) was used in the next step without further
27 purification.
28
29
30
31
32
33
34
35
36
37
38

39 To a pre-dried microwave vial under argon were added crude amine (17 mg), NBD-Cl (17.3
40 mg, 87 μmol), NaHCO_3 (9.8 mg, 117 μmol) and the reactants were dissolved in dry MeOH (0.7
41 mL). The vial was capped, protected from light, and stirred at 50 °C for 4 h. The reaction was
42 cooled to rt, concentrated under a flow of N_2 , redissolved in a mixture of EtOAc (2 mL) and
43 water (2 mL), extracted with EtOAc (x3), washed with brine, and concentrated *in vacuo*. The
44 crude product was purified on preparative HPLC using a Phenomenex Luna C18 5 μm column
45 (250×21.2 mm), with gradient elution of 0.05% TFA/MeCN and 0.05% TFA/ H_2O at a flow rate
46 of 20 mL/min. HPLC fractions were combined and concentrated under reduced pressure and the
47
48
49
50
51
52
53
54
55
56
57
58
59
60

1
2
3 remaining aqueous phase extracted with EtOAc (x5). The organic phases were combined,
4
5 washed with brine and concentrated *in vacuo* to give **4** as a red sticky oil (10.1 mg, 38% over 2
6
7 steps): $R_f = 0.32$ (DCM [10% MeOH]); $^1\text{H NMR}$ (400 MHz, CDCl_3) δ 8.39 (d, $J = 8.4$ Hz, 1H),
8
9 8.01 – 7.92 (m, 1H), 7.84 – 7.77 (m, 1H), 7.72 – 7.67 (m, 1H), 7.63 (d, $J = 7.7$ Hz, 2H), 7.42 –
10
11 7.36 (m, 1H), 7.36 – 7.29 (m, 2H), 7.28 – 7.24 (m, 1H), 7.23 (br s, 1H), 6.01 (d, $J = 8.4$ Hz, 1H),
12
13 4.67 – 4.58 (m, 1H), 4.36 – 4.25 (m, 1H), 4.21 – 3.99 (m, 3H), 3.68 – 3.63 (m, 2H), 3.51 – 3.22
14
15 (m, 6H), 2.58 – 2.45 (m, 1H), 2.39 – 2.17 (m, 4H), 1.94 – 1.73 (m, 4H), 1.70 – 1.55 (m, 2H);
16
17 ESI-HRMS calcd for $\text{C}_{36}\text{H}_{37}\text{F}_3\text{N}_7\text{O}_6\text{S}$ ($\text{M} + \text{H}^+$) 752.2473, found 752.2502; HPLC: $t_R = 12.29$
18
19 min, 99.9% pure.

20
21
22 ***tert*-Butyl (3-(4-(1-(2-(benzo[*b*]thiophen-3-yl)acetyl)-2-methyl-*N*-(4-(trifluoromethyl)-**
23
24 **benzyl)azetidine-2-carboxamido)butanamido)propyl)carbamate (**7**)**. The crude carboxylic
25
26 acid **2** (40.0 mg, 75 μmol) in dry DCM (150 μL) was added Et_3N (20 μL , 0.15 mmol) followed
27
28 by BOP-Cl (23.9 mg, 94 μmol), and the reaction was heated slowly to 50 $^\circ\text{C}$. After 3 h,
29
30 additional Et_3N (25 μL , 0.19 mmol) was added followed by *tert*-butyl (3-aminopropyl)carbamate
31
32 (17.3 mg, 1.0 mmol). The reaction was stirred at 50 $^\circ\text{C}$ for 30 min, cooled to rt, and stirred over
33
34 night before concentration *in vacuo* and purification of the crude product by flash
35
36 chromatography (DCM [5% MeOH]) to yield the desired product as clear sticky oil (23.9 mg,
37
38 46%): $R_f = 0.12$ (DCM [5% MeOH]); $^1\text{H NMR}$ (400 MHz, CDCl_3) δ 7.93 – 7.51 (m, 4H), 7.49 –
39
40 7.13 (m, 5H), 7.24 – 7.11 (m, 1H), 6.79 – 6.40 (m, 1H), 4.92 – 4.49 (m, 2H), 4.47 – 4.27 (m,
41
42 1H), 4.24 – 3.84 (m, 3H), 3.78 – 3.38 (m, 2H), 3.26 – 3.16 (m, 2H), 3.14 – 3.00 (m, 2H), 2.58 –
43
44 2.41 (m, 1H), 2.38 – 2.20 (m, 1H), 1.94 – 1.73 (m, 5H), 1.71 – 1.48 (m, 4H), 1.43* (s, 9H'), 1.42
45
46 (s, 9H''); ESI-HRMS calcd for $\text{C}_{35}\text{H}_{43}\text{F}_3\text{N}_4\text{NaO}_5\text{S}$ ($\text{M} + \text{Na}^+$) 711.2798, found 711.2786.
47
48
49
50
51
52
53
54
55
56
57
58
59
60

Characterization of absorption and fluorescence properties of **4**

Single concentration absorption and fluorescence spectra of fluorescent tracer **4** were recorded at 8.82 μM . Extinction coefficient for **4** in *n*-octanol was recorded in duplicates using a FLUOstar Omega Microplate Reader (BMG labtech). For fluorescent quantum yield determination, fluorescence spectra for **4** were recorded in duplicates using a ChronosFD time-resolved spectrofluorometer coupled to PMT detectors. Coumarin 153 (C-153) and **4** were excited at a fixed excitation wavelength of 402 nm, and C-153 in EtOH was used as an internal standard for determination of quantum yield ($\Phi_{\text{C-153}} = 0.546$, $\lambda_{\text{ex}} = 402$ nm).³⁴ All experiments were performed at 25 °C. Data analysis was performed using Graphpad Prism v5.

IP1 accumulation assay

All IP1 experiments were performed using Flp-InTM T-RExTM 293 cells able to express receptor constructs of interest in an inducible manner. Experiments were carried out using a homogeneous time-resolved FRET-based detection kit (Cis-Bio Bioassays, Codolet, France) according to the manufacturer's protocol. Cells were induced to express the receptor of interest by treatment for 24 h with 100 ng/mL doxycycline and plated at 7500 cells/well in low-volume 384-well plates. The ability of C3 to induce accumulation of IP1 was assessed following a co-incubation for 2 hours with C3, which was preceded by a 15-min pre-incubation with antagonist to allow for equilibration.

Radioligand displacement assay

All receptor radioligand binding experiments using [³H]-**1** were conducted in glass tubes, in binding buffer (50 mM Tris-HCl, 100 mM NaCl, 10 mM MgCl₂, 1 mM EDTA, pH 7.4).

1
2
3 Membrane protein was generated from Flp-InTM T-RExTM 293 cells induced to express the
4 receptor construct of interest with 100 ng/mL doxycycline. For [³H]-**1** competition binding
5 assays, the radioligand at approximately K_d concentration and varying concentrations of
6 unlabeled ligand of choice were co-added to 5 μ g of membrane protein. Non-specific binding of
7 the radioligand was determined in the presence of 10 μ M **8**. After an incubation period of 2 h at
8 25 °C, bound and free [³H]-**1** were separated by rapid vacuum filtration through GF/C glass
9 filters using a 24-well Brandel cell harvester (Alpha Biotech, Glasgow, UK), and unbound
10 radioligand was washed from filters by three washes with ice-cold PBS. After drying (3–12 h), 3
11 mL of Ultima GoldTM XR (PerkinElmer Life Sciences) was added to each sample vial, and
12 radioactivity was quantified by liquid scintillation spectrometry. Aliquots of [³H]-**1** were also
13 quantified to define the concentration of [³H]-**1** added per tube. Data were fitted to a one-site
14 model using Graphpad Prism v6 and used to calculate pK_i values based on a K_d value for [³H]-
15 **1** of 7.5 nM.¹⁶

36 **Equilibrium BRET binding assay**

37
38 The NLuc-hFFA2 construct and cell line were developed as described by Christiansen *et al.*²⁰
39 NLuc-hFFA2 Flp-InTM T-RExTM 293 cells were induced to express the receptor construct by
40 treating with 100 ng/mL doxycycline for 24 h. Cells were then harvested and used to make total
41 cell membrane preparations. Membranes were suspended in binding buffer and transferred into a
42 white 96-well plate at 5 μ g membrane protein per well. Membranes were then co-incubated with
43 the indicated concentration of **4** (and **1** for non-specific binding measurements; or competing
44 ligand for competition experiments) for 2 h at 30 °C. Following incubation, the NLuc substrate,
45 Nano-Glo (Promega) was added to a final 1:800 dilution. Membranes were incubated a further 5
46
47
48
49
50
51
52
53
54
55
56
57
58
59
60

1
2
3 min before the bioluminescent emission at 460 and 545 nm was measured using a Clariostar
4 plate reader (BMG labtech). Total and non-specific saturation binding data were then globally fit
5
6 to a one-site binding model using Graphpad Prism v6. Competition binding experiments were fit
7
8 to a one-site model and used to calculate pK_i values based on a K_d value for **4** of 65.1 nM.
9
10
11

12 13 14 15 **Kinetic BRET binding assay**

16
17 For kinetic BRET binding assays, cell membranes were generated as for the equilibrium
18 binding assay and again distributed in white 96-well microplates (2.5 μ g membrane
19 protein/well). The Nano-Glo substrate was then added (1:800 final dilution) before incubation
20
21 for 5 min at 30 °C. Plates were then inserted into a Clariostar plate reader, with temperature set
22 to 30 °C and set to read emission at 460 and 545 nm at 90 s intervals. For association
23
24 experiments, **4** was manually added to the plate after 60 s to a final concentration of 100, 300,
25
26 500 or 1000 nM. Readings were continued at 90 s intervals for the indicated time period. For
27 dissociation experiments the reaction was pre-incubated for 2 h at 30 °C followed by two washes
28
29 with binding buffer, performed via centrifugation at 14,000 rpm at 4 °C for 15 min. The pellet
30
31 was then resuspended in binding buffer at 37 °C and transferred into a white 96-well microplate
32
33 at 90 μ L/well and standard kinetic binding assay procedure as described above was followed. In
34
35 all kinetic experiments parallel wells were assessed in which **1** had been pre-added, and these
36
37 were used to subtract the non-specific binding signal for **4**. Kinetic binding data were then fit to
38
39 one-phase association or dissociation models using Graphpad Prism v6 to obtain estimates of k_{off} ,
40
41 k_{on} , and K_d .
42
43
44
45
46
47
48
49
50
51
52
53
54
55
56
57
58
59
60

Determination of the “On” and “Off” Rates of Unlabeled Ligands through Measurement of Competition Binding Kinetics of **4**

The kinetic binding parameters of unlabeled ligands were determined through assessment of the binding kinetics of **4** as described above. Here the standard procedure was followed. After 5 min pre-incubation of membrane protein with Nano-Glo, **4** (100 nM) and the competing unlabeled ligand at three different concentrations (1-, 3-, or 10-fold the estimated respective K_i concentration) were added simultaneously. Readings were then continued at 90 s intervals for 60 min. Three different concentrations of competitor were assessed to ensure that the rate parameters calculated were independent of ligand concentration. Data were fit globally using the kinetics of the competitive binding equation available from GraphPad Prism v6, with the k_{on} and k_{off} values of **4** entered as constraints.

AUTHOR INFORMATION

Corresponding Author

*Tel: +45 6550 2568. E-mail: ulven@sdu.dk

Author Contributions

The manuscript was written through contributions of all authors. All authors have given approval to the final version of the manuscript. [§]These authors contributed equally.

Funding Sources

The study has been funded by the Danish Council for Strategic Research (grant 11-116196) and the University of Southern Denmark. EC is supported by a fellowship from the Lundbeck Foundation. BDH is supported by a fellowship from the University of Glasgow.

ABBREVIATIONS

BOP-Cl, bis(2-oxo-3-oxazolidinyl)phosphinic chloride; BRET, bioluminescence resonance energy transfer; FFA1, free fatty acid receptor 1 (GPR40); FFA2, free fatty acid receptor 2 (GPR43); FFA3, free fatty acid receptor 2 (GPR41); NBD, 4-nitro-7-aminobenzodiazole; NLuc, NanoLuciferase; PE, petroleum ether; PMT, photomultiplier tubes; SS, Stoke's shift.

REFERENCES

- (1) Topping, D. L.; Clifton, P. M. Short-chain fatty acids and human colonic function: Roles of resistant starch and nonstarch polysaccharides. *Physiol. Rev.* **2001**, *81*, 1031-1064.
- (2) Offermanns, S. Free fatty acid (FFA) and hydroxy carboxylic acid (HCA) receptors. *Annu. Rev. Pharmacol. Toxicol.* **2014**, *54*, 407-434.
- (3) Ulven, T. Short-chain free fatty acid receptors FFA2/GPR43 and FFA3/GPR41 as new potential therapeutic targets. *Front. Endocrinol.* **2012**, *3*, 111.
- (4) Milligan, G.; Bolognini, D.; Sergeev, E. Ligands at the free fatty acid receptors 2/3 (GPR43/GPR41). *Handb. Exp. Pharmacol.* **2017**, *236*, 17-32.
- (5) Milligan, G.; Shimpukade, B.; Ulven, T.; Hudson, B. D. Complex pharmacology of free fatty acid receptors. *Chem. Rev.* **2017**, *117*, 67-110.
- (6) Ge, H.; Li, X.; Weiszmann, J.; Wang, P.; Baribault, H.; Chen, J.-L.; Tian, H.; Li, Y. Activation of G protein-coupled receptor 43 in adipocytes leads to inhibition of lipolysis and suppression of plasma free fatty acids. *Endocrinology* **2008**, *149*, 4519-4526.

- 1
2
3
4 (7) Tang, C.; Ahmed, K.; Gille, A.; Lu, S.; Grone, H. J.; Tunaru, S.; Offermanns, S. Loss of
5 FFA2 and FFA3 increases insulin secretion and improves glucose tolerance in type 2
6 diabetes. *Nat. Med.* **2015**, *21*, 173-177.
7
8
9
10 (8) Brown, A. J.; Goldsworthy, S. M.; Barnes, A. A.; Eilert, M. M.; Tcheang, L.; Daniels, D.;
11 Muir, A. I.; Wigglesworth, M. J.; Kinghorn, I.; Fraser, N. J.; Pike, N. B.; Strum, J. C.;
12 Steplewski, K. M.; Murdock, P. R.; Holder, J. C.; Marshall, F. H.; Szekeres, P. G.;
13 Wilson, S.; Ignar, D. M.; Foord, S. M.; Wise, A.; Dowell, S. J. The orphan G protein-
14 coupled receptors GPR41 and GPR43 are activated by propionate and other short chain
15 carboxylic acids. *J. Biol. Chem.* **2003**, *278*, 11312-11319.
16
17
18 (9) Maslowski, K. M.; Vieira, A. T.; Ng, A.; Kranich, J.; Sierro, F.; Yu, D.; Schilter, H. C.;
19 Rolph, M. S.; Mackay, F.; Artis, D.; Xavier, R. J.; Teixeira, M. M.; Mackay, C. R.
20 Regulation of inflammatory responses by gut microbiota and chemoattractant receptor
21 GPR43. *Nature* **2009**, *461*, 1282-1287.
22
23
24 (10) Vinolo, M. A. R.; Ferguson, G. J.; Kulkarni, S.; Damoulakis, G.; Anderson, K.;
25 Bohlooly-Y, M.; Stephens, L.; Hawkins, P. T.; Curi, R. SCFAs induce mouse neutrophil
26 chemotaxis through the GPR43 receptor. *PLoS One* **2011**, *6*, e21205.
27
28
29 (11) Bjorkman, L.; Martensson, J.; Winther, M.; Gabl, M.; Holdfeldt, A.; Uhrbom, M.;
30 Bylund, J.; Hojgaard Hansen, A.; Pandey, S. K.; Ulven, T.; Forsman, H.; Dahlgren, C.
31 The neutrophil response induced by an agonist for free fatty acid receptor 2 (GPR43) is
32 primed by tumor necrosis factor alpha and by receptor uncoupling from the cytoskeleton
33 but attenuated by tissue recruitment. *Mol. Cell. Biol.* **2016**, *36*, 2583-2595.
34
35
36 (12) Forbes, S.; Stafford, S.; Coope, G.; Heffron, H.; Real, K.; Newman, R.; Davenport, R.;
37 Barnes, M.; Grosse, J.; Cox, H. Selective FFA2 agonism appears to act via intestinal
38
39
40
41
42
43
44
45
46
47
48
49
50
51
52
53
54
55
56
57
58
59
60

- 1
2
3 PYY to reduce transit and food intake but does not improve glucose tolerance in mouse
4 models. *Diabetes* **2015**, *64*, 3763-3771.
- 5
6
7
8 (13) Pizzonero, M.; Dupont, S.; Babel, M.; Beaumont, S.; Bienvenu, N.; Blanque, R.; Cherel,
9 L.; Christophe, T.; Crescenzi, B.; De Lemos, E.; Delerive, P.; Deprez, P.; De Vos, S.;
10 Djata, F.; Fletcher, S.; Kopiejewski, S.; L'Ebraly, C.; Lefrancois, J. M.; Lavazais, S.;
11 Manioc, M.; Nelles, L.; Oste, L.; Polancec, D.; Quenehen, V.; Soulas, F.; Triballeau, N.;
12 van der Aar, E. M.; Vandeghinste, N.; Wakselman, E.; Brys, R.; Saniere, L. Discovery
13 and optimization of an azetidine chemical series as a free fatty acid receptor 2 (FFA2)
14 antagonist: From hit to clinic. *J. Med. Chem.* **2014**, *57*, 10044-10057.
- 15
16
17
18 (14) Ang, Z.; Ding, J. L. GPR41 and GPR43 in obesity and inflammation - protective or
19 causative? *Front. Immunol.* **2016**, *7*, 28.
- 20
21
22
23 (15) Kimura, I.; Ozawa, K.; Inoue, D.; Imamura, T.; Kimura, K.; Maeda, T.; Terasawa, K.;
24 Kashihara, D.; Hirano, K.; Tani, T.; Takahashi, T.; Miyauchi, S.; Shioi, G.; Inoue, H.;
25 Tsujimoto, G. The gut microbiota suppresses insulin-mediated fat accumulation via the
26 short-chain fatty acid receptor GPR43. *Nat. Commun.* **2013**, *4*, 1829.
- 27
28
29
30 (16) Namour, F.; Galien, R.; Van Kaem, T.; Van der Aa, A.; Vanhoutte, F.; Beetens, J.; Van't
31 Klooster, G. Safety, pharmacokinetics and pharmacodynamics of GLPG0974, a potent
32 and selective FFA2 antagonist, in healthy male subjects. *Br. J. Clin. Pharmacol.* **2016**,
33 *82*, 139-148.
- 34
35
36
37 (17) Vermeire, S.; Kojecký, V.; Knoflíček, V.; Reinisch, W.; Kaem, T. V.; Namour, F.;
38 Beetens, J.; Vanhoutte, F. GLPG0974, an FFA2 antagonist, in ulcerative colitis: efficacy
39 and safety in a multicenter proof-of-concept study. *J. Crohn's Colitis* **2015**, *Suppl 1*, S39.
- 40
41
42
43
44
45
46
47
48
49
50
51
52
53
54
55
56
57
58
59
60

- 1
2
3
4
5
6
7
8
9
10
11
12
13
14
15
16
17
18
19
20
21
22
23
24
25
26
27
28
29
30
31
32
33
34
35
36
37
38
39
40
41
42
43
44
45
46
47
48
49
50
51
52
53
54
55
56
57
58
59
60
- (18) Vernall, A. J.; Hill, S. J.; Kellam, B. The evolving small-molecule fluorescent-conjugate toolbox for Class A GPCRs. *Br. J. Pharmacol.* **2014**, *171*, 1073-1084.
- (19) Ma, Z.; Du, L.; Li, M. Toward fluorescent probes for G-protein-coupled receptors (GPCRs). *J. Med. Chem.* **2014**, *57*, 8187-8203.
- (20) Heisig, F.; Gollos, S.; Freudenthal, S. J.; El-Tayeb, A.; Iqbal, J.; Muller, C. E. Synthesis of BODIPY derivatives substituted with various bioconjugatable linker groups: a construction kit for fluorescent labeling of receptor ligands. *J. Fluoresc.* **2014**, *24*, 213-230.
- (21) Christiansen, E.; Hudson, B. D.; Hansen, A. H.; Milligan, G.; Ulven, T. Development and characterization of a potent free fatty acid receptor 1 (FFA1) fluorescent tracer. *J. Med. Chem.* **2016**, *59*, 4849-4858.
- (22) Yates, A. S.; Doughty, S. W.; Kendall, D. A.; Kellam, B. Chemical modification of the naphthoyl 3-position of JWH-015: in search of a fluorescent probe to the cannabinoid CB2 receptor. *Bioorg. Med. Chem. Lett.* **2005**, *15*, 3758-3762.
- (23) Petrov, R. R.; Ferrini, M. E.; Jaffar, Z.; Thompson, C. M.; Roberts, K.; Diaz, P. Design and evaluation of a novel fluorescent CB2 ligand as probe for receptor visualization in immune cells. *Bioorg. Med. Chem. Lett.* **2011**, *21*, 5859-5862.
- (24) Haldar, S.; Chattopadhyay, A. Application of NBD-labeled lipids in membrane and cell biology. *Springer Ser. Fluoresc.* **2013**, *13*, 37-50.
- (25) Barresi, E.; Bruno, A.; Taliani, S.; Cosconati, S.; Da Pozzo, E.; Salerno, S.; Simorini, F.; Daniele, S.; Giacomelli, C.; Marini, A. M.; La Motta, C.; Marinelli, L.; Cosimelli, B.; Novellino, E.; Greco, G.; Da Settimo, F.; Martini, C. Deepening the topology of the

- 1
2
3 translocator protein binding site by novel N,N-dialkyl-2-arylindol-3-ylglyoxylamides. *J.*
4
5
6 *Med. Chem.* **2015**, *58*, 6081-6092.
- 7
8 (26) Lin, S.; Struve, W. S. Time-resolved fluorescence of nitrobenzoxadiazole-aminohexanoic
9
10 acid: effect of intermolecular hydrogen-bonding on non-radiative decay. *Photochem.*
11
12 *Photobiol.* **1991**, *54*, 361-365.
- 13
14 (27) Stoddart, L. A.; Johnstone, E. K.; Wheal, A. J.; Goulding, J.; Robers, M. B.; Machleidt,
15
16 T.; Wood, K. V.; Hill, S. J.; Pflieger, K. D. Application of BRET to monitor ligand
17
18 binding to GPCRs. *Nat. Methods* **2015**, *12*, 661-663.
- 19
20 (28) Wüstner, D.; Christensen, T.; Solanko, L.; Sage, D. Photobleaching Kinetics and Time-
21
22 Integrated Emission of Fluorescent Probes in Cellular Membranes. *Molecules* **2014**, *19*,
23
24 11096.
- 25
26 (29) Sergeev, E.; Hansen, A. H.; Pandey, S. K.; MacKenzie, A. E.; Hudson, B. D.; Ulven, T.;
27
28 Milligan, G. Non-equivalence of key positively charged residues of the free fatty acid 2
29
30 receptor in the recognition and function of agonist versus antagonist ligands. *J. Biol.*
31
32 *Chem.* **2016**, *291*, 303-317.
- 33
34 (30) Tikhonova, I.; Poerio, E. Free fatty acid receptors: structural models and elucidation of
35
36 ligand binding interactions. *BMC Struct. Biol.* **2015**, *15*, 16.
- 37
38 (31) Dowling, M. R.; Charlton, S. J. Quantifying the association and dissociation rates of
39
40 unlabelled antagonists at the muscarinic M3 receptor. *Br. J. Pharmacol.* **2006**, *148*, 927-
41
42 937.
- 43
44 (32) Brantis, C. E.; Ooms, F.; Bernard, J. Novel amino acid derivatives and their use as
45
46 GPR43 receptor modulators. *PCT Int. Appl. WO2011092284* **2011**.
- 47
48
49
50
51
52
53
54
55
56
57
58
59
60

- 1
2
3 (33) Hudson, B. D.; Tikhonova, I. G.; Pandey, S. K.; Ulven, T.; Milligan, G. Extracellular
4 ionic locks determine variation in constitutive activity and ligand potency between
5 species orthologs of the free fatty acid receptors FFA2 and FFA3. *J. Biol. Chem.* **2012**,
6 287, 41195-41209.
7
8
9
10
11
12 (34) Rurack, K.; Spieles, M. Fluorescence quantum yields of a series of red and near-infrared
13 dyes emitting at 600-1000 nm. *Anal. Chem.* **2011**, 83, 1232-1242.
14
15
16
17
18
19
20
21
22
23
24
25
26
27
28
29
30
31
32
33
34
35
36
37
38
39
40
41
42
43
44
45
46
47
48
49
50
51
52
53
54
55
56
57
58
59
60

TABLE OF CONTENT GRAPHICS

